Improvements in radiographic and clinical assessment of distal radius fracture healing by FE-estimated bone stiffness

Phillip J.C. Spanswick [a,c], Danielle E. Whittier [a,c], Cory Kwong [b], Robert Korley [b], Steven K. Boyd [a,c], Prism S. Schneider [b,c,*]

[a] Department of Radiology, Cumming School of Medicine, University of Calgary, Calgary, Canada
[b] Department of Surgery, Division of Orthopaedic Trauma, Cumming School of Medicine, University of Calgary, Calgary, AB, Canada
[c] McCaig Institute for Bone and Joint Health, University of Calgary, Calgary, Canada

ARTICLE INFO

ABSTRACT

Bone strength determined from finite element (FE) modelling provides an estimate of fracture healing progression following a distal radius fracture (DRF), but how these measures relate to patient-reported outcomes and functional outcomes remains unknown. We hypothesized that changes in bone stiffness and bone mineral density measured using high-resolution peripheral quantitative computed tomography (HR-pQCT) are associated with clinically available measures of functional and patient-reported outcomes. We also aimed to identify which clinical outcome measures best predict fracture stiffness and could therefore be used to inform cast removal.

Participants ($n = 30$) with stable distal radius fractures were followed for two week intervals from the time of fracture until two months post-fracture, then at three months and six months post-fracture. At each follow-up, participants underwent clinical, radiographic, and functional assessments, as well as had their fractured wrist scanned using HR-pQCT. Recovery of bone stiffness during fracture healing was determined from micro-FE (µFE) models generated from HR-pQCT image data.

During the DRF healing process, significant longitudinal changes were found in µFE-estimated stiffness, patient-reported outcomes, grip strength, range of motion (ROM), tenderness, number of cortices healed based on radiographs, and fracture line visibility ($p < 0.05$); however, no significant change was detected in HR-pQCT based total bone mineral density. Patient-reported outcomes, such as the Patient-Rated Wrist Evaluation (PRWE) and the Quick Disability of the Arm, Shoulder and Hand (QuickDASH) questionnaire, correlated strongly with µFE-estimated stiffness ($0.61 \geq r_m \geq 0.66$). Based on µFE-estimated stiffness, PRWE and QuickDASH are the best predictors of stiffness recovery ($p < 0.05$) and may be used to guide duration of cast immobilization in the clinical setting.

1. Introduction

Distal radius fractures (DRF) are common injuries, accounting for up to 20% of all fractures presenting to the emergency department (Armstrong et al., 2019a). Closed reduction and cast immobilization is the most common treatment for these fractures. For example, a recent study found that 84% of DRFs were treated with cast immobilization (Armstrong et al., 2019b). Despite the prevalence of these injuries, clinical practice guidelines are lacking to direct optimal duration of cast immobilization. Serial clinical and radiographic assessments are typically completed to evaluate healing progression, yet several studies have reported a lack of consensus regarding criteria used to define fracture

union (*J Chiropr Med*, 2017; Bhandari et al., 2002; Bhandari et al., 2012; Morshed, 2014; Whelan et al., 2010). Restoration of bone strength and stiffness are important outcomes following fracture healing, but predicting fracture stiffness from radiographs is sensitive to errors (Panjabi et al., 1985) and measuring stiffness in the clinical setting is difficult. In a study using manual assessment of models representing mid-shaft diaphyseal fractures, there was a propensity towards over estimating fracture stiffness (Webb et al., 1996). Recently, finite element (FE) methods coupled with advanced imaging have enabled stiffness to be estimated *in vivo* and several clinical studies implementing high-resolution peripheral quantitative computed tomography (HR-pQCT) imaging have demonstrated the feasibility of assessing longitudinal

changes in stiffness, bone density, and microarchitecture following a DRF (de Jong et al., 2014; de Jong et al., 2016; Heyer et al., 2019).

Functional outcomes such as improved grip strength and range of motion (ROM) are considered indicators of healing progression. Grip strength and ROM also correlate highly with patient satisfaction following a DRF (Arora et al., 2009; Fujii et al., 2002) and can be quantified in the clinical setting with high reliability (Horger, 1990; Mathiowetz, 2002; Mathiowetz et al., 1984). Patient-reported outcomes including the Patient-Rated Wrist Evaluation (PRWE) and the Quick Disability of the Arm, Shoulder and Hand (QuickDASH) questionnaire are reliable tools commonly used in clinical practice to evaluate pain and disability in the wrist and upper limb, respectively (Gummesson et al., 2003; MacDermid et al., 1998). These tools have been used extensively to capture pain and functional outcomes across a variety of functional activities, following a DRF (Swart et al., 2012; Tsang et al., 2017). Associations between microarchitecture and long-term functional outcomes have been reported (Meyer et al., 2014); however, serial clinical measures of wrist pain, function, and disability have not been compared with HR-pQCT analysis during fracture healing. We investigated clinical outcomes including pain and function, as well as fracture stiffness, and total volumetric bone mineral density (Tt.BMD) in patients with DRFs treated with cast immobilization.

We hypothesized that longitudinal changes for *in vivo* measures of stiffness and Tt.BMD are associated with clinically available measures of functional and patient-reported outcomes. Our primary objective was to compare clinical outcome measurements of fracture healing evaluation with changes in stiffness and Tt.BMD measures based on HR-pQCT in men and women up to six months following a DRF treated with cast immobilization.

2. Methods

2.1. Participants

Following approval by the Conjoint Health Research Ethics Board at the University of Calgary (REB16-0032), participants were identified during the initial assessment at the Foothills Medical Center (FMC) Cast Clinic located in Calgary, Canada. Eligibility criteria included participants 18 years of age or older, with an acute stable DRF with a non-operative treatment plan, who were able to complete the first follow-up within 21 days of their initial injury. Exclusion criteria stipulated that participants did not have a pre-existing wrist injury or deformity on either side, a concomitant injury, a known metabolic bone disease, a history of rheumatoid arthritis or other inflammatory arthropathy, were not being treated for osteoporosis, or were on chronic corticosteroid treatment for three months or more. Participants who satisfied the inclusion and exclusion criteria signed a written informed consent to participate and underwent standard of care treatment. If late crossover from non-operative to operative treatment occurred due to fracture displacement, the participant was excluded. Upon enrollment into the study, demographic data were collected from participants including age,

height, weight, body mass index (BMI), sex, activity level, past medical history, handedness, occupation, and mechanism of injury. Participants completed follow-up at 2, 4, 6, 8, 12, 26 weeks post-fracture. A summary of the measurements taken at each timepoint is illustrated in Table 1. A senior orthopaedic resident classified fractures using the AO Foundation/Orthopaedic Trauma Association (AO/OTA) Classification of Fractures and grouped similar fracture patterns together according to the classification type (extra-articular, partial articular, and complete articular) (Meinberg et al., 2018).

2.2. HR-pQCT image acquisition

At each follow-up, the fractured radius was scanned using high-resolution peripheral quantitative computed tomography (HR-pQCT, XtremeCT II, Scanco Medical, Brüttisellen, Switzerland). A scan of the contralateral, uninjured wrist was also completed at baseline, to represent pre-fracture conditions. A previous study in our lab reported differences in microarchitecture and failure load between the dominant and non-dominant radius were less than 3% (Hildebrandt et al., 2016). The length and location of the fracture was marked on the anteroposterior x-ray by the attending surgeon, which was used to guide the selection of the appropriate scan length. A reference line was placed on the endplate of the distal radius, and the scan region extended proximally 20.4 mm (336 slices; Fig. 1). If the fractures extended further in the proximal direction, the scan region was extended to 30.6 mm (504 slices). Scans were performed with 68 kVp effective energy, 1.47 mA intensity and 43 ms integration time at 61 μm isotropic voxel resolution. The wrist being scanned was immobilized in a standardized carbon fibre holder to reduce motion during the scan. All scans acquired prior to cast removal were completed with the plaster or fibreglass cast on. At the end of the required immobilization treatment, the cast was removed and scans were acquired without a cast. Grey-scale density values were scaled using conversion equations developed in our lab to correct for beam hardening effects due to overlying plaster or fibreglass casts (Whittier et al., 2019).

2.3. HR-pQCT image processing

All scans were graded for motion artifacts from a scale of one (no motion) to five (significant blurring and discontinuities) by a single rater. Those with a motion score of four or greater were removed from analysis (Pauchard et al., 2012). Scans were also graded for motion between stacks using a previously reported scoring system from one (no stack shift) to three (severe stack offset), where scans with a score of three were removed from analysis (Spanswick et al., 2020). The periosteal surface was semi-automatically contoured (Image Processing Language, v6.6, Scanco Medical AG, Brüttisellen, Switzerland). A total bone mask was defined based on the periosteal surface of the bone and was the basis for assessing total volumetric bone mineral density (Tt. BMD). Tt.BMD at the fractured radius was compared to Tt.BMD at the unfractured radius to determine relative change.

Table 1
Data acquisition timeline.

Outcome measure	Pre-FX	Initial	2 week (±7 days)	4 week (±7 days)	6 week (±7 days)	8 week (±7 days)	12 week (±7 days)	26 week (±3 week)
PRWE	✓	✓	✓	✓	✓	✓	✓	✓
QuickDASH	✓	✓	✓	✓	✓	✓	✓	✓
VAS	✓	✓	✓	✓	✓	✓	✓	✓
Range of motion					✓	✓	✓	✓
Grip strength					✓	✓	✓	✓
Tenderness					✓	✓	✓	✓
X-Ray		✓	✓	✓	✓	✓	✓	✓
HR-pQCT			✓	✓	✓	✓	✓	✓
HR-pQCT, contralateral			✓					

Abbreviations: VAS, visual analog scale; PRWE, Patient Reported Wrist/Hand Evaluation; QuickDASH, Quick Disability of the Arm, Shoulder, and Hand.
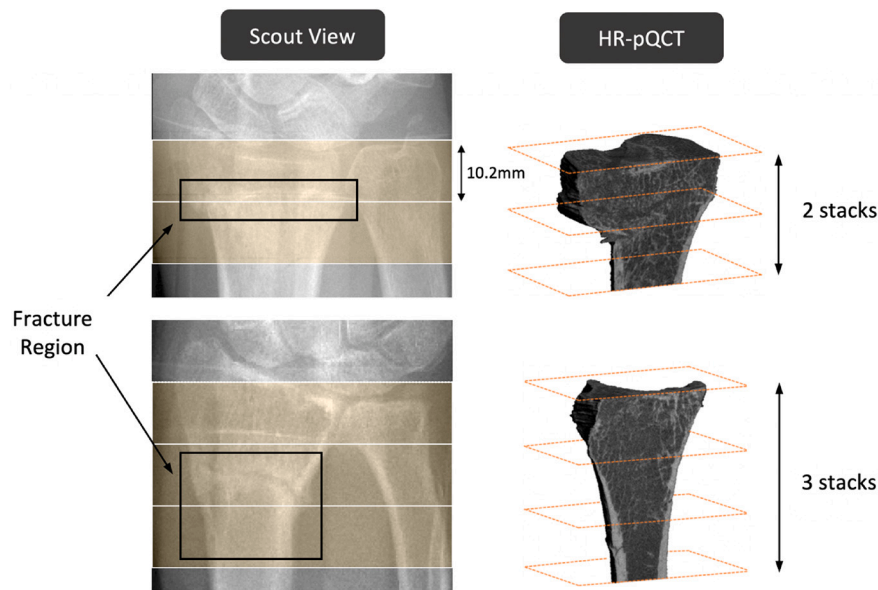
Fig. 1. Scout view and HR-pQCT images of distal radius fractures illustrating two and three stack regions of interest highlighted in orange. The image with a two stack region of interest contains 336 slices in total. The image with a three stack region of interest contains 504 slices in total. The fracture line is outlined with a box in each scout view image.

2.4. Finite element modelling

Homogeneous modulus micro-FE (µFE) models were generated, which we have previously shown to effectively capture changes in stiffness during fracture healing (Spanswick et al., 2020). Image voxels were converted directly to 8-node hexahedral elements. A global threshold of 320 mgHA/cm^3 was used to segment the bone. All bone was assumed linear elastic and isotropic; a Poisson's ratio of 0.3 and a homogeneous elastic modulus of 8748 MPa were assigned for the bone tissue properties (Whittier et al., 2018). Uniaxial compression and torsional loading tests were performed. For uniaxial compression, the distal surface nodes were selected on the articular surface of the bone and constrained in the axial direction (z-axis), while the proximal surface was displaced 0.1 mm in compression. For torsional loading, the distal articular surface was fully constrained and the proximal surface was rotated 1° about the z-axis and crossing through the center of mass of the model. Nodal displacements were determined using a custom FE solver (Faim v8.0, Numerics88 Solutions Ltd.), and apparent stiffness was calculated from total nodal force and mean nodal displacement. Stiffness of the contralateral, uninjured wrist was used to represent baseline conditions and changes in stiffness was estimated as the percent difference in stiffness at each timepoint compared to baseline.

2.5. Patient-reported outcomes

At each follow-up, participants completed validated questionnaires designed to measure pain, disability, and function following a DRF. Questionnaires included the Patient Reported Wrist Evaluation (PRWE) – a reliable measure of patient-rated pain and disability (MacDermid et al., 1998) – and the Quick Disability of the Arm, Shoulder and Hand (QuickDASH) questionnaire – which has demonstrated high reliability to assess outcomes following DRF (MacDermid, 1996). Participants self-reported their degree of pain during the previous week using a standardized visual analog scale (VAS). At the time of initial assessment and study enrollment, participants completed the questionnaires for both their pre-injury status, as well as based on their current post-injury symptoms. Each outcome measure is reported as change from the baseline, pre-injury state.

2.6. Functional outcomes

At the end of the required immobilization treatment, the cast was removed and functional measurements were taken to determine movement, strength, and pain. Tenderness at the fracture site was determined by direct palpation over the fracture site by the attending surgeon and reported as either present or absent. Range of motion was measured for wrist flexion, extension, pronation, supination, ulnar deviation, and radial deviation. The summation of within plane movement was used to determine an arc of motion, for example wrist flexion and extension were summed to determine an arc of motion within the sagittal plane. Range of motion was calculated as a percentage of the contralateral wrist to determine restoration of ROM as the outcome parameter. Grip strength was measured with three sequential trials of each hand using a handgrip dynamometer (Jamar Hydraulic Hand Dynamometer, Sammons Preston Inc.). The mean of the three trials was expressed as a percentage of the contralateral hand grip strength.

2.7. Radiographic assessment

Anteroposterior (AP) and lateral radiographs were acquired at each follow-up. Fractures were classified by a senior orthopaedic resident using the AO Foundation/Orthopaedic Trauma Association (AO/OTA) Classification of Fractures (Meinberg et al., 2018) based on this initial injury radiographs. Beginning at the four week follow-up assessment, radiographs were scored by the treating surgeon. Fracture line visibility and cortical continuity were determined: the two most common criteria for assessing fracture union at the radius (Corrales et al., 2008). The number of healed cortices (volar, dorsal, ulnar, radial) was determined based on the AP and lateral wrist radiographs. Fracture line visibility was determined (no change = 0, radiodensity increased = 1, fading = 2, and healed = 3), and measurements from the AP and lateral wrist radiographs were summed, providing a total score from zero to six.

2.8. Statistical analysis

Descriptive statistics were analyzed. A mixed effects analysis of temporal change in HR-pQCT based parameters, patient-reported, functional, and radiographic outcomes was performed with R (Version 3.5.2) and lme4 (Version 1.1.20). An empty means intercept model was

initially fit to determine the variance attributed to between- and within-person differences. Linear, quadratic, and piecewise unconditional models were tested, then time-invariant predictors were added including age (centered to the mean age), fracture type, sex, and hand dominance; the interaction of each fixed effect with time was tested. A Wald test was used to determine significance of individual fixed effects and maximum log likelihood ($-2*$log likelihood ($-2LL$)) statistics were used to determine significance of random effects between nested models; the level of statistical significance was set to $p < 0.05$. Model fit was checked graphically using plots of transformed residuals. For piecewise models, the point where the slope of the model changed (transition point) was determined using an optimizer to minimize the deviance of the fitted model conditional upon the transition point.

Repeated measures correlation was calculated with R (Version3.5.2) and the "rmcorr" package (Version 0.3.0), to determine the association for paired measures, reported as the repeated measures correlation coefficient (r_m). Strength of association was interpreted according to Mukaka et al. (Mukaka, 2012): 0.0 to 0.3, negligible; 0.3 to 0.5, weak; 0.5 to 0.7 moderate; 0.7 to 0.9, strong; 0.9 to 1.0 very strong. Clinical measures that correlated strongly with *in vivo* measurements were tested as time-variant predictors of stiffness. A correlation between the actuals and predicted stiffness values was used to determine if clinical parameters accounted for variance in predicted stiffness outcomes.

3. Results

We enrolled 37 participants with a stable DRF with a minimum of six month follow-up (Fig. 2). Five participants were lost to follow-up and two crossed over into surgical treatment, the remaining participants were followed until six months post-fracture ($n = 30$). Most participants were female ($n = 27$; 90%), six males were recruited, however only three completed six month follow-up (Table 2). Participant age within our cohort was evenly distributed, with 9 participants 18–39 years old, 11 participants 40–59 years old, and 10 participants 60–90 years old. The non-dominant wrist was fractured nearly twice as often ($n = 19$) compared with the dominant wrist ($n = 11$).

We found significant longitudinal changes in patient-reported

Table 2
Cohort, injury, and treatment characteristics, means ± standard deviation (min, max), or number (%).

| Demographics	
Age [years]	51.8 ± 16.5 (19.4, 84.3)
Male	3 (10.0%)
Female	27 (90.0%)
BMI [kg/m^2]	25.4 ± 4.4 (19.8, 33.9)
FX on the dominant limb	11 (36.7%)
Activity level	
Employed (active)	12 (40.0%)
Employed (sedentary)	5 (16.7%)
Unemployed	2 (6.7%)
Student	2 (6.7%)
Retired (active)	8 (26.7%)
Retired (sedentary)	0 (0%)
Mechanism of injury	
Ground level fall	10 (33.3%)
Fall from height greater than 3 ft	2 (6.7%)
Sports related injury	16 (53.3%)
Other	2 (6.7%)
Fracture type	
A (extraarticular)	15 (50.0%)
B (partial articular)	1 (3.3%)
C (complete articular)	14 (46.7%)
Cast immobilization	
Duration in cast [weeks]	6.1 ± 1.3 (4, 8)
Splint required	14.0 (46.7%)
Duration in splint [weeks]	2.0 ± 2.5 (0, 8)
Cast thickness (mm)	3.9 ± 1.1 (2.1, 6.2)

Abbreviations: BMI, body mass index; FX, fracture.

outcomes, functional outcomes, radiographic outcomes, and μFE-estimated stiffness over the six months post-fracture ($p < 0.05$). No significant change in Tt.BMD was found ($p > 0.3$). Time series plots for stiffness, PRWE, grip strength, cortical healing, and Tt.BMD are presented (Fig. 3) and results for mixed effects models summarized (Table 3).

QuickDASH, VAS, ROM, tenderness, and fracture line visibility
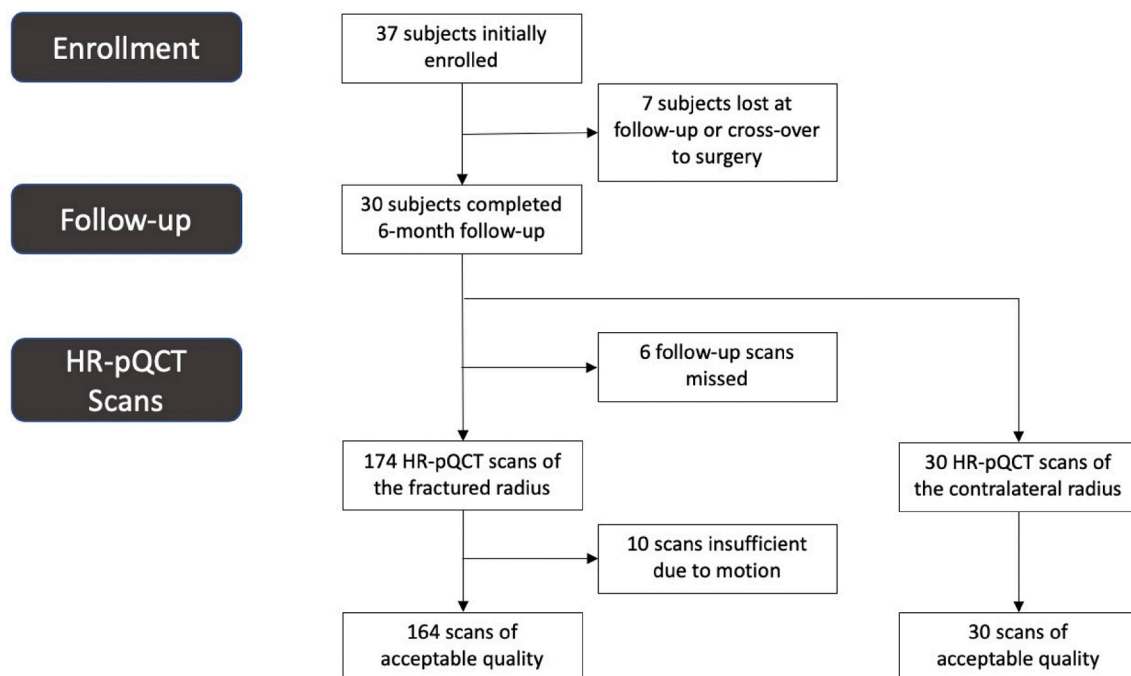
Fig. 2. Overview of participant recruitment, follow-up rate, and HR-pQCT scans rejection/acceptance for analysis. Six scans were rejected from analysis due to intrastack motion and four were rejected due to inter-stack motion.
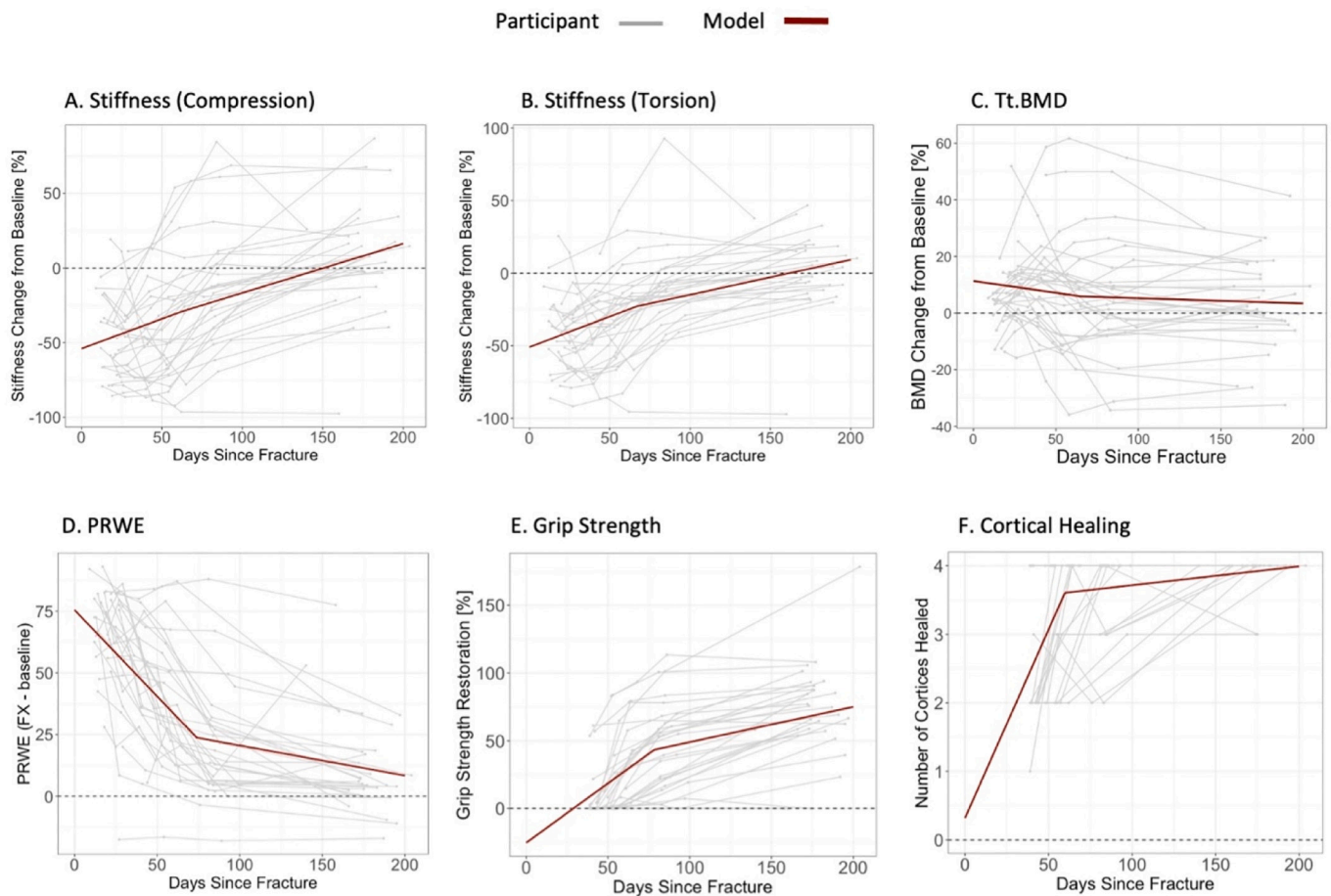
Fig. 3. Time series plots for HR-pQCT- and FE-derived parameters, PRWE, Grip Strength, and cortical healing outcomes, illustrating individual participants (grey) and mixed effects model (red) trajectories.

Table 3
Coefficients with 95% confidence intervals for the final mixed effects models (HR-pQCT and FE-derived parameters, PRWE, grip strength, and cortical healing).

| Variable | Stiffness | | HR-pQCT | Patient reported and functional outcomes | | Radiographic outcomes |
	Compression	Torsion	Tt.BMD	PRWE	Grip strength	Cortical healing
Intercept	−54.28* (−73.41, −35.15)	−51.44* (−64.73, −38.15)	11.3 (3.6, 19.0)	75.5* (67.7, 83.2)	−25.2* (−35.6, 14.8)	0.32* (0.09, 0.55)
TP (days)	63	71	65	74	78	60
Days < TP	0.41* (0.09, 0.73)	0.43* (0.21, 0.65)	−0.08 (−0.24, 0.08)	−0.71* (−0.87, −0.55)	0.91* (0.66, 1.16)	0.06* (0.03, 0.08)
Days > TP	0.33* (0.22, 0.44)	0.23* (0.13, 0.33)	−0.01 (−0.06, 0.02)	−0.12* (−0.18, −0.05)	0.26* (0.17, 0.34)	3.0e-2* (2.9e-3, 5.3e-2)
Sex (Male)				−32.3* (−45.4, −7.4)	38.1* (17.57, 58.22)	
Age					−1.01* (−1.61, −0.42)	
Age * Days < TP					−0.02* (−0.04, −0.01)	
Hand dominance	17.11* (−33.03, −1.19)	14.31* (−33.27, −1.82)				

Notes: Data presented as coefficient (95% confidence interval). Coefficients for the fixed effect hand dominance are describing fractures to the dominant limb. For models including age, sex and/or hand dominance, the Intercept refers to the mean value for a 51 year old female with a non-dominant limb fracture.
Abbreviations: TP, transition point (the point where the slope changes for the piecewise models).
* Denotes values that are significant ($p < 0.05$).

outcomes are reported in the supplemental figures and tables (Fig. S6 and Table S6). Moderate to strong correlations ($0.61 \geq r_m \geq 0.72$) were found comparing grip strength; range of motion including flexion/extension, pronation/supination, and ulnar/radial deviation; PRWE scores; and QuickDASH scores with µFE-estimated stiffness (Table 4). PRWE and QuickDASH outcomes were found to be negative predictors

of µFE-estimated stiffness and stiffness recovery (Table 5), accounting for an additional 5% and 10% of the variance in stiffness, respectively (p < 0.05). Grip strength was a predictor of stiffness when modeled separately; however, it was no longer significant when PRWE or QuickDASH were included as co-variants. Weak correlations ($0.46 \geq r_m \geq 0.50$) were found between radiographic outcomes and change in stiffness.

Table 4

Repeated measures correlations between stiffness parameters, patient reported outcomes, functional outcomes, and radiographic outcomes.

	Stiffness	
	Compression [r_m]	Torsion [r_m]
Patient reported outcomes		
PRWE change	−0.62* (−0.77, −0.59)	−0.66* (−0.75, −0.55)
QuickDASH change	−0.62* (0.76, −0.56)	−0.61* (−0.71, −0.49)
VAS change	−0.38* (0.56, −0.28)	−0.31* (0.46, 0.14)
Functional outcomes		
ROM (flexion/extension)	0.68* (0.54, 0.78)	0.69* (0.56, 0.79)
ROM (pronation/supination)	0.63* (0.48, 0.75)	0.66* (0.52, 0.77)
ROM (ulnar/radial deviation)	0.66* (0.51, 0.77)	0.63* (0.47, 0.75)
Grip strength	0.69* (0.55, 0.79)	0.71* (0.58, 0.81)
Tenderness	−0.30* (−0.49, −0.08)	−0.33 (−0.52, −0.12)
Radiographic outcomes		
Cortices healed	0.46* (0.25, 0.63)	0.50* (0.30, 0.66)
Fracture line visibility	0.46* (0.25, 0.63)	0.49* (0.29, 0.65)

Notes: Data presented as repeated measures correlation coefficients (95% confidence interval).
Abbreviations: ROM, range of motion; PRWE, patient rated wrist/hand evaluation; VAS, visual analog scale; r_m, repeated measures correlation (bounded by −1 to 1); QuickDASH, Quick Disability of the Arm, Shoulder, and Hand.
* Denotes values that are significant ($p < 0.05$).

During the first six weeks post-fracture (the mean time of cast immobilization), the piecewise mixed effects models showed a rapid recovery (17% increase) in μFE-estimated stiffness that was concurrent with PRWE improvement (41% decrease) within the same timeframe. Additionally, piecewise mixed effects model of radiographic outcomes showed an increase of 2–3 healed cortices within the first six weeks. During later stages of fracture healing, recovery slowed, with an average 2% increase per week in stiffness and a functional improvement of 1% per week based on PRWE. Hand dominance significantly affected stiffness, such that fractures of the non-dominant wrist had a greater reduction in stiffness (compression, −17%; torsion, −14%; p < 0.05) (relative to the contralateral, uninjured wrist) than fractures that occurred on the dominant wrist. In our cohort of 30 patients, neither age, fracture type, nor sex were found to significantly predict stiffness. At the time of cast removal (mean = 6 weeks ±1.3), grip strength was only 10% of the baseline estimate from the contralateral, uninjured wrist. By six months post-fracture only half of participants recovered up to 75% of their baseline grip strength. Age affected grip strength, with

each increase in age of 10 years resulting in a decreased mean grip strength of 10% and decreased rate of grip strength recovery of 1.4% per week. Age also affected ulnar/radial deviation, with each increase in age of 10 years resulting in a decreased mean ulnar/radial deviation of 5%.

4. Discussion

Our findings illustrate that stiffness, patient-reported outcomes, and functional outcomes had recovered considerably by six weeks post-fracture (the mean time of cast immobilization); stiffness of the fractured radius had increased to a deficit of 37% compared to the contralateral wrist and PRWE and QuickDASH scores were within 50 points of baseline (Fig. 4). Stiffness recovery to within 40% of the contralateral may serve as a benchmark indicating cast removal. PRWE and Quick-DASH correlated strongly on a patient level with *in vivo* stiffness measures and predicted stiffness recovery, indicating they may direct duration of cast immobilization in the clinical setting. Pain and radiographic outcomes including tenderness, VAS, cortical healing, and fracture line visibility displayed improvement throughout the healing process; however, they had weaker associations with *in vivo* stiffness, suggesting that they are less valuable as tools to inform cast removal.

Patients who present with poor pain and disability (PRWE, Quick-DASH > 50 above baseline, where a higher score indicates increased pain and dysfunction) likely do not have sufficient restoration of mechanical stiffness at the fracture site and should continue with cast immobilization. Alternatively, patients who present improved pain and disability (PRWE, QuickDASH within 50 points of their baseline) may indicate fracture healing progression and cast removal. The removal of casts potentially several weeks earlier than the mean 6 week timepoint could enable patients to return to work and recreational activities sooner. Previous studies have demonstrated earlier cast removal may be safe (Christensen et al., 1995; Jensen et al., 1997), including a recent study that found no difference in pain or functional outcome for minimally displaced DRFs that were immobilized for three *versus* five weeks (Bentohami et al., 2019).

As our study followed the standard of care at the FMC, we were unable to verify the use of PRWE or QuickDASH outcomes to inform cast removal. To verify the benchmark values presented in Fig. 4, future studies may investigate the outcome of patients who have their cast removed at different levels of pain and disability recovery. Evaluating the outcome of patients who have their cast removed when they recover to within 50, 40, or 30 points of baseline PRWE or QuickDASH would
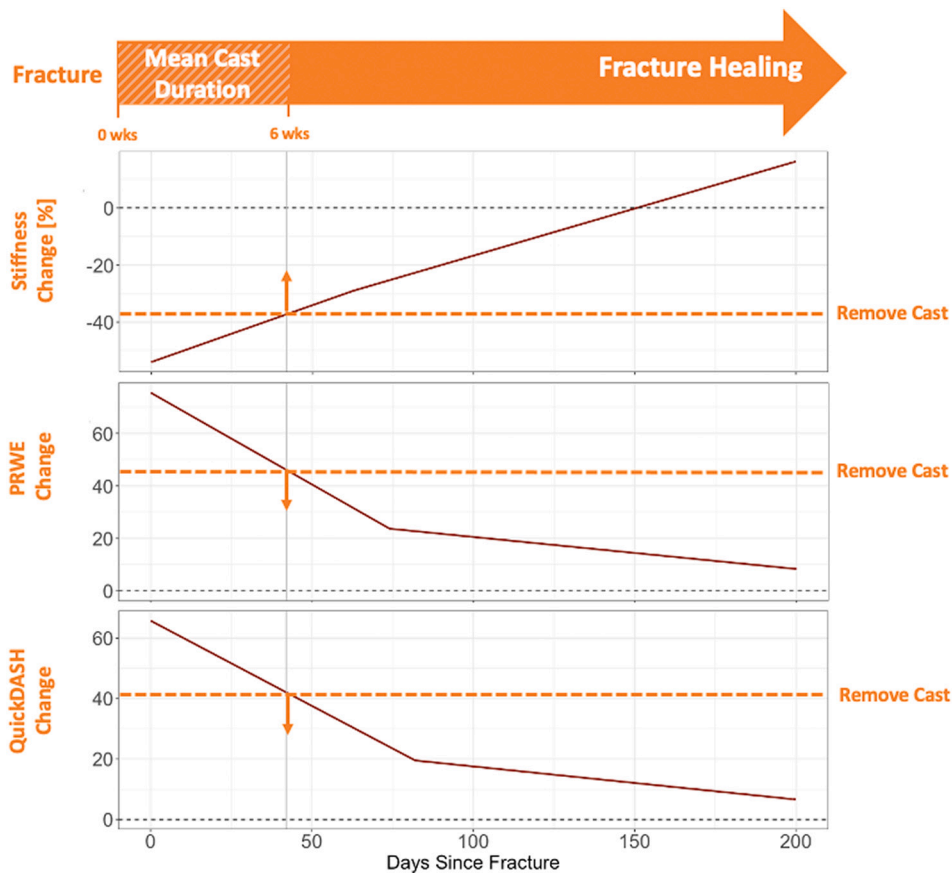
Table 5

Coefficients with 95% confidence intervals for the mixed effects models (unconditional models and models with QuickDASH or PRWE as a time-variant predictor).

Variable	Unconditional growth model		Add QuickDASH and piecewise time interaction		Add PRWE and piecewise time interaction	
	Compression	Torsion	Compression	Torsion	Compression	Torsion
Intercept	−54.27*	−51.44*	−58.89*	−54.82*	−65.23*	−56.48*
	(−69.53, −39.01)	(−63.23, −39.64)	(−74.12, −43.66)	(−67.78, −41.85)	(−81.41, −49.04)	(−70.27, −42.69)
TP (days)	63	71	63	71	63	71
Days < TP	0.40*	0.42*	0.75*	0.67*	0.93*	0.78*
	(0.08, 0.73)	(0.21, 0.65)	(0.22, 1.28)	(0.27, 1.08)	(0.41, 1.46)	(0.38, 1.18)
Days > TP	0.33*	0.23*	0.20*	0.13*	0.17*	0.10
	(0.21, 0.44)	(0.13, 0.33)	(0.08, 0.33)	(4.9e-3, 0.25)	(0.03, 0.30)	(−0.03, 0.21)
QuickDASH			−0.60*	−0.52*		
			(−0.84, −0.36)	(−0.77, −0.24)		
QuickDASH * Days < TP			−0.01*	−0.01*		
			(−0.02, −5.30e-3)	(−0.02, 2.7e-3)		
PRWE					−0.71*	−0.67*
					(−0.92, −0.48)	(−0.92, −0.41)
PRWE * Days < TP					−0.02*	−0.01*
					(−0.01, −2.5e-3)	(−0.02, −0.01)

Notes: Data presented as coefficient (95% confidence interval). For models including PRWE or QuickDASH, the intercept refers to the mean value for baseline (pre-fracture) PRWE or QuickDASH values.
Abbreviations: TP, transition point (the point where the slope changes for the piecewise models); PRWE, patient rated wrist/hand evaluation; QuickDASH, Quick Disability of the Arm, Shoulder, and Hand.
* Denotes values that are significant ($p < 0.05$).

Fig. 4. Guidelines for stiffness and clinical instruments that may be used to direct duration of cast immobilization. The red line indicates the mixed effects models for each outcome parameter.

provide a better indication of the optimum benchmark to direct duration of cast immobilization in the clinical setting.

PRWE and QuickDASH outcomes illustrated a high degree of similarity in terms of the trajectory of the piecewise models and the strong correlation with *in vivo* stiffness. Both outcomes were also predictors of stiffness and rate of stiffness recovery, indicating they are valuable tools to inform fracture healing progression and should be included in the determination of cast removal. This supports previously reported associations between long-term PRWE and QuickDASH outcomes and early changes in torsional stiffness (Meyer et al., 2014). PRWE and Quick-DASH are easily implemented in the clinical setting, they demonstrate near identical responsiveness (Tsang et al., 2017), and have good content validity and reliability for the assessment of patients with distal radius fractures (Kleinlugtenbelt et al., 2018). Pain scores, as determined from the VAS, correlated weakly with *in vivo* stiffness, suggesting that it is not a valuable tool for predicting fracture strength. Previous studies have highlighted limits of the VAS as a serial measures of pain and reliability in determining long-term outcomes following a DRF (Noback et al., 2015; Langley and Sheppeard, 1985), suggesting multiitem pain questionnaires, such as PRWE or QuickDASH, may be a preferable alternative.

Grip strength and range of motion are routinely used clinical measures of functional recovery after fracture, as both have high predictive value for patient satisfaction following a DRF (Arora et al., 2009; Fujii et al., 2002). Both were strongly associated with stiffness, but only grip strength was found to predict mean change in stiffness (Table S7). When PRWE or QuickDASH scores were included as co-variants, neither grip strength nor range of motion predicted stiffness. This may be attributed to a lack of power due to our relatively small sample size, but it suggests that PRWE and QuickDASH are stronger predictors of fracture stiffness

and may be preferable instruments to guide duration of cast immobilization. This is supported by a previous study that found no association between early changes in torsional stiffness and long-term range of motion outcome (Meyer et al., 2014). The weak correlation between tenderness at the fracture site and stiffness may be attributed to the perception of pain being highly influenced by a multitude of factors including individual and cultural differences in pain perception and tolerance (Morshed, 2014). Several participants continued to report tenderness at the six month follow-up, when all casts were removed, indicating that tenderness may be capturing aspects of healing that can be attributed to associated soft tissue injury and unrelated to the bone status directly; bringing into question its value as an instrument to inform duration of cast immobilization.

Radiographic outcomes including cortical healing (ulnar, volar, dorsal, radial cortex) and fracture line visibility scores were obtained beginning at the four week follow-up assessment. There were several cases where the number of healed cortices decreased or the visibility of the fracture line increased in subsequent assessments. This may be due to bone resorption at the fracture site, a normal part of the fracture healing process (Cox et al., 2010), which manifests as increased radiolucency at the fracture site. It may also be attributed to inaccuracies with scoring, as radiographic scores were not necessarily determined by the same surgeon at each follow-up. Previous studies have reported poor reliability in determining fracture union or fracture stability with planar radiographic assessment (Hammer et al., 1985; Davis et al., 2004; Blokhuis et al., 2001). While radiography is a useful tool to evaluate fracture reduction and anatomical alignment, the difficulty and lack of consistency in scoring planar radiographs highlights limitations as a tool to accurately define fracture union and direct duration of cast immobilization.

The serial HR-pQCT images illustrated dramatic changes in bone structure (Fig. 5); changes in microarchitecture and morphology, including cortical geometry, trabecular density, and callus volume, were apparent from visual assessment of HR-pQCT images. It is likely that Tt. BMD is not able to capture these structural changes, as it is a global parameter calculated from the whole bone. A number of limitations may contribute to this lack of sensitivity. First, defining the periosteal contour is subjective. Automatically generated contours generally require little correction for intact bone, but automatically generated contours of fractured bone often need large portions to be manually corrected, which makes maintaining consistency across multiple scans for multiple participants challenging. Second, the formation of periosteal callus and displacement of bone fragments considerably changes the cross-sectional area across sequential scans. Third, Tt.BMD does not distinguish compartmental changes in density, which have previously been captured to describe localized changes in bone structure (de Jong et al., 2014). We were unable to determine compartmental density or microarchitectural parameters, as overlapping cortical fragments and disrupted trabecular bone severely limited our ability to define the endosteal contour.

Several limitations were present in this study. The enrollment rate was lower than predicted, therefore there was a relatively small sample size. There was an underrepresentation of males, which, although was clinically representative of presenting eligible patients, may affect the generalizability of our results and likely the power to detect sex differences in fracture healing progression. The precision of μFE-estimated stiffness values is reduced by repositioning error. This error was minimized through standardized procedures for positioning participants in the scanner and our two medical imaging technologists using the fracture line that was measured on the planar anteroposterior radiograph. Scoring of the planar x-rays was not necessarily completed by the same surgeon at each follow-up, therefore inter-rater differences are introduced as a potential source of error. Finally, while significant longitudinal changes in stiffness were captured throughout the fracture healing process, these models cannot be validated against mechanical testing. The μFE models may consider adjacent fractured bone to be erroneously connected leading to an overestimation of stiffness; this phenomena was previously reported by Arias-Moreno et al. (Arias-Moreno et al., 2016).

It is recommended that future studies focus on more effective methods to segment cortical and trabecular compartments. This may improve the consistency of periosteal contours and allow compartmental densities and microarchitectural parameters to be obtained. In addition, a more comprehensive x-ray scoring protocol would be beneficial, including more raters with a range of experience and multiple scoring timepoints. This would allow the reliability of different scoring criteria within and between raters to be evaluated. We also recommend that future work focuses on improving the precision of the μFE models by reducing repositioning error through image registration. We were unable to apply whole bone 3D image registration due to large differences in bone structure across follow-up scans; however, new image registration techniques have been developed to register individual bone fragments accounting for inter-fragmentary displacement (de Jong et al., 2017).

In conclusion, recovery of μFE-estimated stiffness, PRWE, and QuickDASH may be used to inform radiographic and clinical assessment following a DRF and for guiding the time required for cast immobilization. PRWE and QuickDASH were strongly associated with *in vivo* fracture stiffness, they significantly predicted rate of stiffness recovery following a DRF, and they are easily implemented in the clinical setting. Radiographic outcomes (cortical healing and fracture line visibility) and pain metrics (VAS and tenderness to palpation at the fracture site) offer less value as a measure of healing progression due to inconsistencies in scoring and weak correlation with *in vivo* stiffness, respectively. Recovery of *in vivo* stiffness provides an objective measure of fracture healing progression, informing duration of cast immobilization, and clinical fracture assessment instruments.

CRediT authorship contribution statement

Phillip J.C. Spanswick: Conceptualization, Methodology, Formal analysis, Data curation, Writing – original draft. **Danielle E. Whittier:** Data curation, Writing – review & editing. **Cory Kwong:** Conceptualization, Investigation, Data curation, Writing – review & editing. **Robert Korley:** Investigation, Data curation, Writing – review & editing. **Steven**
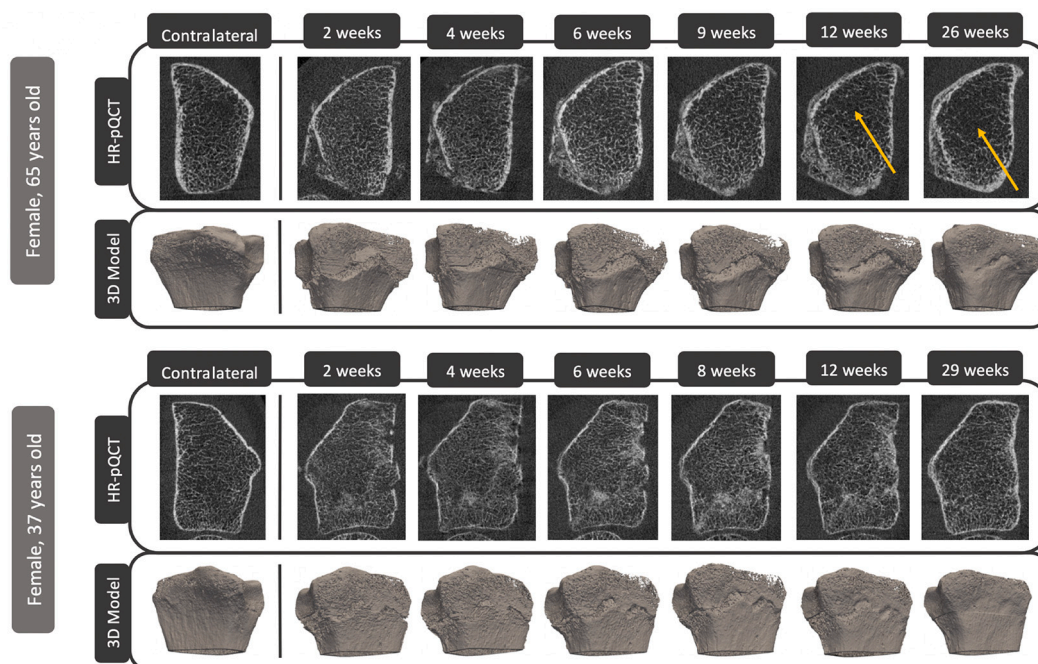
Fig. 5. Longitudinal HR-pQCT axial slices (slice 202) and segmented 3D models. The series on the top row is a 65 year old female; considerable trabecular bone loss is evident from HR-QCT images in later follow-ups (indicated by the orange arrows), and the fracture line is clear from the 3D models throughout. The series on the bottom row is a 37 year old female; at the six month follow-up the fractured bone appears to resemble the pre-fracture state.

K. Boyd: Conceptualization, Methodology, Writing – review & editing.
Prism S. Schneider: Conceptualization, Methodology, Investigation, Data curation, Writing – review & editing.

Appendix A. Supplementary data

Supplementary data to this article can be found online at https://doi.org/10.1016/j.bonr.2021.100748.

References

Arias-Moreno, A.J., Ito, K., van Rietbergen, B., Sep 6 2016. Micro-Finite Element analysis will overestimate the compressive stiffness of fractured cancellous bone. J Biomech 49 (13), 2613–2618. https://doi.org/10.1016/j.jbiomech.2016.05.021.

Armstrong, K.A., von Schroeder, H.P., Baxter, N.N., et al., 2019a. Stable rates of operative treatment of distal radius fractures in Ontario, Canada: a population-based retrospective cohort study (2004–2013). Can J Surg 62 (6), 016218 (Sep 23). https://doi.org/10.1503/cjs.016218.

Armstrong, K.A., von Schroeder, H.P., Baxter, N.N., et al., 2019b. Stable rates of operative treatment of distal radius fractures in Ontario, Canada: a population-based retrospective cohort study (2004–2013). Can J Surg 62 (6), 386–392 (Dec 1). https://doi.org/10.1503/cjs.016218.

Arora, R., Gabl, M., Gschwentner, M., et al., 2009. A comparative study of clinical and radiologic outcomes of unstable colles type distal radius fractures in patients older than 70 years: nonoperative treatment versus volar locking plating. J. Orthop. Trauma 23 (4), 237–242.

Bentohami, A., van Delft, E.A.K., Vermeulen, J., et al., Feb 2019. Non- or minimally displaced distal radial fractures in adult patients: three weeks versus five weeks of cast immobilization-a randomized controlled trial. J Wrist Surg 8 (1), 43–48. https://doi.org/10.1055/s-0038-1668155.

Bhandari, H.M., Guyatt, F.G., Swiontkowski, H.M., et al., 2002. A lack of consensus in the assessment of fracture healing among Orthopaedic surgeons. J. Orthop. Trauma 16 (8), 562–566. https://doi.org/10.1097/00005131-200209000-00004.

Bhandari, M., Fong, K., Sprague, S., et al., 2012. Variability in the definition and perceived causes of delayed unions and nonunions: a cross-sectional, multinational survey of orthopaedic surgeons. JBJS 94 (15), e109.

Blokhuis, T.J., de Bruine, J.H., Bramer, J.A., et al., Mar 2001. The reliability of plain radiography in experimental fracture healing. Skelet. Radiol. 30 (3), 151–156. https://doi.org/10.1007/s002560000317.

Christensen, O.M., Christiansen, T.G., Krasheninnikoff, M., Hansen, F.F., 1995. Length of immobilisation after fractures of the distal radius. Int. Orthop. 19 (1), 26–29. https://doi.org/10.1007/bf00184910.

Corrales, A.L., Morshed, A.S., Bhandari, A.M., Miclau, A.T., 2008. Variability in the assessment of fracture-healing in Orthopaedic trauma studies. The Journal of Bone & Joint Surgery 90 (9), 1862–1868. https://doi.org/10.2106/JBJS.G.01580.

Cox, G., Einhorn, T.A., Tzioupis, C., Giannoudis, P.V., Mar 2010. Bone-turnover markers in fracture healing. J Bone Joint Surg Br 92 (3), 329–334. https://doi.org/10.1302/0301-620X.92B3.22787.

Davis, B.J., Roberts, P.J., Moorcroft, C.I., et al., Jun 2004. Reliability of radiographs in defining union of internally fixed fractures. Injury 35 (6), 557–561. https://doi.org/10.1016/S0020-1383(03)00262-6.

de Jong, J.J., Willems, P.C., Arts, J.J., et al., Jul 2014. Assessment of the healing process in distal radius fractures by high resolution peripheral quantitative computed tomography. Bone 64, 65–74. https://doi.org/10.1016/j.bone.2014.03.043.

de Jong, J.J.A., Heyer, F.L., Arts, J.J.C., et al., May 2016. Fracture repair in the distal radius in postmenopausal women: a follow-up 2 years postfracture using HRpQCT. J. Bone Miner. Res. 31 (5), 1114–1122. https://doi.org/10.1002/jbmr.2766.

de Jong, J.J.A., Christen, P., Plett, R.M., et al., 2017. Feasibility of rigid 3D image registration of high-resolution peripheral quantitative computed tomography images of healing distal radius fractures. PLoS One 12 (7), e0179413. https://doi.org/10.1371/journal.pone.0179413.

Fujii, K., Henmi, T., Kanematsu, Y., et al., Jun 2002. Fractures of the distal end of radius in elderly patients: a comparative study of anatomical and functional results. J Orthop Surg (Hong Kong) 10 (1), 9–15. https://doi.org/10.1177/230949900201000103.

Gummesson, C., Atroshi, I., Ekdahl, C., Jun 16 2003. The disabilities of the arm, shoulder and hand (DASH) outcome questionnaire: longitudinal construct validity and measuring self-rated health change after surgery. BMC Musculoskelet Disord 4, 11. https://doi.org/10.1186/1471-2474-4-11.

Hammer, R.R., Hammerby, S., Lindholm, B., Oct 1985. Accuracy of radiologic assessment of tibial shaft fracture union in humans. Clin Orthop Relat Res (199), 233–238 [Online]. Available. https://www.ncbi.nlm.nih.gov/pubmed/4042484.

Heyer, F.L., de Jong, J.J.A., Willems, P.C., et al., Oct 2019. Long-term functional outcome of distal radius fractures is associated with early post-fracture bone stiffness of the fracture region: an HR-pQCT exploratory study. Bone 127, 510–516. https://doi.org/10.1016/j.bone.2019.06.013.

Hildebrandt, E.M., Manske, S.L., Hanley, D.A., Boyd, S.K., Apr-Jun 2016. Bilateral asymmetry of radius and tibia bone macroarchitecture and microarchitecture: a high-resolution peripheral quantitative computed tomography study. J. Clin. Densitom. 19 (2), 250–254. https://doi.org/10.1016/j.jocd.2015.02.005.

Horger, M.M., Apr 1990. The reliability of goniometric measurements of active and passive wrist motions. Am. J. Occup. Ther. 44 (4), 342–348. https://doi.org/10.5014/ajot.44.4.342.

"Erratum to "A Guideline of Selecting and Reporting Intraclass Correlation Coefficients for Reliability Research" [J Chiropr Med 2016;15(2):155–163]," J Chiropr Med 16 (4), Dec 2017, 346. https://doi.org/10.1016/j.jcm.2017.10.001.

Jensen, M.R., Andersen, K.H., Jensen, C.H., 1997. Management of undisplaced or minimally displaced Colles' fracture: one or three weeks of immobilization. J. Orthop. Sci. 2 (6), 424–427.

Kleinlugtenbelt, Y.V., Krol, R.G., Bhandari, M., et al., Jan 2018. Are the patient-rated wrist evaluation (PRWE) and the disabilities of the arm, shoulder and hand (DASH) questionnaire used in distal radial fractures truly valid and reliable? Bone Joint Res 7 (1), 36–45. https://doi.org/10.1302/2046-3758.71.BJR-2017-0081.R1.

Langley, G.B., Sheppeard, H., 1985. The visual analog scale - its use in pain measurement (in English). Rheumatol Int 5 (4), 145–148. https://doi.org/10.1007/Bf00541514.

MacDermid, J.C., Apr-Jun 1996. Development of a scale for patient rating of wrist pain and disability. J. Hand Ther. 9 (2), 178–183. https://doi.org/10.1016/s0894-1130(96)80076-7.

MacDermid, C.J., Turgeon, S.T., Richards, H.R., et al., 1998. Patient rating of wrist pain and disability: a reliable and valid measurement tool. J. Orthop. Trauma 12 (8), 577–586. https://doi.org/10.1097/00005131-199811000-00009.

Mathiowetz, V., 2002. Comparison of Rolyan and Jamar dynamometers for measuring grip strength. Occup. Ther. Int. 9 (3), 201–209. https://doi.org/10.1002/oti.165.

Mathiowetz, V., Weber, K., Volland, G., Kashman, N., Mar 1984. Reliability and validity of grip and pinch strength evaluations. J Hand Surg Am 9 (2), 222–226. https://doi.org/10.1016/s0363-5023(84)80146-x.

Meinberg, E., Agel, J., Roberts, C., et al., 2018. Fracture and dislocation classification compendium—2018. J. Orthop. Trauma 32, S1–S10.

Meyer, U., De Jong, J.J., Bours, S.G., et al., 2014. Early changes in bone density, microarchitecture, bone resorption, and inflammation predict the clinical outcome 12 weeks after conservatively treated distal radius fractures: an exploratory study. J. Bone Miner. Res. 29 (9), 2065–2073. https://doi.org/10.1002/jbmr.2225.

Morshed, S., 2014. Current options for determining fracture union. Advances in Medicine 2014. https://doi.org/10.1155/2014/708574.

Mukaka, M.M., Sep 2012. Statistics corner: a guide to appropriate use of Correlation coefficient in medical research (in English). Malawi Med J 24 (3), 69–71 [Online]. Available: https://www.ncbi.nlm.nih.gov/pmc/articles/PMC3576830/pdf/MMJ2403-0069.pdf.

Noback, P., Cuellar, D., Lombardi, J., et al., 2015. Evaluating pain in orthopedic patients: can the visual analog scale be used as a long-term outcome instrument? J Pain Relief 4 (182), 2.

Panjabi, M.M., Walter, S.D., Karuda, M., et al., 1985. Correlations of radiographic analysis of healing fractures with strength: a statistical analysis of experimental osteotomies. J. Orthop. Res. 3 (2), 212–218. https://doi.org/10.1002/jor.1100030211.

Pauchard, Y., Liphardt, A.M., Macdonald, H.M., et al., Jun 2012. Quality control for bone quality parameters affected by subject motion in high-resolution peripheral quantitative computed tomography. Bone 50 (6), 1304–1310. https://doi.org/10.1016/j.bone.2012.03.003.

Spanswick, P.J., Boyd, S.K., Kwong, C., et al., 2020. Restoration of Stiffness During Fracture Healing at the Distal Radius, Using HR-pQCT and Finite Element Methods.

Swart, E., Nellans, K., Rosenwasser, M., May 2012. The effects of pain, supination, and grip strength on patient-rated disability after operatively treated distal radius

fractures. J Hand Surg Am 37 (5), 957–962. https://doi.org/10.1016/j.
jhsa.2012.01.028.

Tsang, P., Walton, D., Grewal, R., MacDermid, J., Jun 2017. Validation of the
QuickDASH and DASH in patients with distal radius fractures through agreement
analysis. Arch Phys Med Rehabil 98 (6), 1217–1222 (e1). https://doi.org/10.1016/j.
apmr.2016.11.023.

Webb, J., Herling, G., Gardner, T., et al., Jun 1996. Manual assessment of fracture
stiffness. Injury 27 (5), 319–320.

Whelan, B.D., Bhandari, D.M., Stephen, H.D., et al., 2010. Development of the
radiographic union score for tibial fractures for the assessment of tibial fracture

healing after intramedullary fixation. The Journal of Trauma: Injury, Infection, and
Critical Care 68 (3), 629–632. https://doi.org/10.1097/TA.0b013e3181a7c16d.

Whittier, D.E., Manske, S.L., Kiel, D.P., et al., 2018. Harmonizing finite element
modelling for non-invasive strength estimation by high-resolution peripheral
quantitative computed tomography. J. Biomech. 80, 63–71. https://doi.org/
10.1016/j.jbiomech.2018.08.030.

Whittier, D.E., Manske, S.L., Boyd, S.K., Schneider, P.S., 2019. The correction of
systematic error due to plaster and fiberglass casts on HR-pQCT bone parameters
measured in vivo at the distal radius. J. Clin. Densitom. 22 (3), 401–408. https://doi.
org/10.1016/j.jocd.2018.11.005.